

Normal-Mode Splitting and Linewidth Averaging for Two-State Atoms in an Optical Cavity

M. G. Raizen

Department of Physics, University of Texas at Austin, Austin, Texas 78712

R. J. Thompson, R. J. Brecha, H. J. Kimble, and H. J. Carmichael^(a)

Norman Bridge Laboratory of Physics 12-33, California Institute of Technology, Pasadena, California 91125

(Received 3 April 1989)

An investigation of the radiative processes for a collection of N two-state atoms strongly coupled to the field of a high-finesse optical cavity is presented. Observations of the spectral response of the composite system to weak external modulation reveal a coupling-induced normal-mode splitting. Linewidth averaging leads to linewidths below the free-space atomic width.

PACS numbers: 42.50.Kb, 32.70.Jz, 42.65.Pc

The radiative processes of atoms in the presence of boundaries such as provided by a resonant cavity have been investigated in recent years within the context of cavity quantum electrodynamics.¹ While the free-space decay of an atom is characterized by the Einstein A -coefficient γ , the interaction of an atom with a cavity introduces three new rates not present for atoms in free space; these rates are the cavity damping rate κ , the decay rate γ' into continuum modes other than those of the cavity, and the coupling rate g , where g characterizes the oscillatory exchange of excitation between the atom and the field of the cavity. For weak coupling of the atom to the resonator ($\gamma' \ll g^2/\kappa \ll \kappa$), large enhancements² and suppressions³ of atomic spontaneous emission have been observed¹ with cavities encompassing a large fraction f of the total 4π solid angle of free space ($\gamma' \ll \gamma$), in agreement with a perturbative description incorporating the cavity-modified density of states. On the other hand, for strong coupling ($g \gg \gamma', \kappa$) the nonperturbative nature of the interaction requires a description not from the viewpoint of the altered radiative processes of the atom or cavity alone, but rather in terms of the dynamics of the composite atom-field entity.^{4,5} While impressive investigations of this underdamped regime have been conducted in the microwave domain with Rydberg atoms for which $g^2/\kappa \gg \kappa \gg \gamma'$,^{6,7} complimentary studies in the optical domain have been largely absent since the coherent coupling rate g is usually dominated either by κ or by γ' . The interest in optical studies arises not only because of the possibility for direct field measurements, but also because of the opportunity for investigations in the strongly coupled regime with atomic dissipation entering as an important process.

Within this context we present in this Letter direct spectroscopic measurements of the normal-mode splitting for the oscillator system formed by the collective atomic polarization of N two-state atoms strongly coupled to a single mode of a high-finesse optical cavity.^{8,9} Although $f \ll 1$ and hence $\gamma' \cong \gamma$, the experiments are nonetheless carried out in a regime for which $g\sqrt{N} \gg \gamma > \kappa$ (with $g\sqrt{N}$ the effective coupling rate in the limit of a weak intracavity field)^{10,11} and hence in a regime for which a photon emitted into the cavity by the

atomic polarization is likely to be absorbed and reemitted many times before it escapes. By recording the spectral response of the composite atom-cavity system to a weak external probe field, we observe a distinctive doublet symmetrically split about the otherwise common frequency of atoms and cavity and find that this normal-mode splitting is in quantitative agreement with the predicted eigenfrequencies over a range of intracavity atomic number $20 \leq N \leq 600$. Our observations at optical frequencies are thus of the vacuum-field Rabi splitting¹² extended from the one-atom case to the situation $N > 1$ and follow in the spirit of previous time-domain investigations of collective atom-cavity oscillations for Rydberg atoms in a microwave cavity.¹³ For each of the two peaks of the split doublet, we also observe subnatural linewidths due to a dynamical linewidth averaging which results from the strong coherent coupling of the collective atomic polarization to the cavity mode.^{5,14} Linewidth reductions of 25% relative to free-space atomic decay are recorded over a wide range of operating conditions. Finally, we explore the behavior of the normal-mode structure as the atomic and cavity resonances are detuned, and observe that the line positions and widths approach values characteristic of decoupled atoms and cavity.

Our starting point is an analysis of the eigenvalue structure for the composite system of N two-state atoms coupled to a single cavity mode. In the limit of weak intracavity field and for coincident cavity resonance frequency ω_C and atomic transition frequency ω_A , the eigenvalues obtained either from the master equation for a single atom¹⁴ or from the Maxwell-Bloch equations for $N \gg 1$ ¹⁰ are $\lambda_0 = -\gamma$ and

$$\lambda_{\pm} = -\frac{1}{4}(2\kappa + \gamma/\Gamma) \pm [\frac{1}{16}(2\kappa - \gamma/\Gamma)^2 - \kappa\gamma C/\Gamma]^{1/2}, \quad (1)$$

where λ_0 gives the decay of the atomic inversion and λ_{\pm} describe the normal modes formed from the intracavity field and the collective atomic polarization. Equation (1) is written in a rotating frame at the common frequency $\omega_C = \omega_A$; $\Gamma \equiv \gamma/2\gamma_{\perp}$ with γ_{\perp} the transverse decay rate; and $C = \Gamma N g^2/\kappa\gamma$ is the atomic cooperativity parameter of optical bistability, with $g = (\mu^2 \omega_C/2\hbar\epsilon_0 V)^{1/2}$,

where μ is the transition dipole moment and V is the effective cavity mode volume. We see that $\text{Im}(\lambda_{\pm})$ (normal-mode splitting) is nonzero for the case $(\kappa\gamma C/\Gamma)^{1/2} = g\sqrt{N} > \frac{1}{4}|2\kappa - \gamma/\Gamma|$, and that in this case $\text{Re}(\lambda_{\pm})$ (normal-mode decay) is an average of cavity and atomic polarization decay rates.^{5,14} For $\kappa < \gamma$, $\text{Re}(\lambda_{\pm})$ is smaller than the spontaneous emission rate in free space, approaching half the natural free-space rate for $\kappa \rightarrow 0$. This linewidth reduction by linewidth averaging results from the strong coherent coupling of atomic and field oscillators, such that for $\kappa \ll \gamma$ atomic excitation can be hidden from decay by residing in the undamped field oscillator 50% of the time. Note that we assume throughout that $f \ll 1$, so that large line splittings and linewidth reductions occur even for the case $\gamma' \approx \gamma$, and that these conclusions are valid for arbitrary $N = 1, 2, 3, \dots$.

Our experimental technique for probing the structure of the atom-field system follows the discussion of Agarwal;¹⁵ we record the spectral response of the system to weak external modulation as the frequency of the modulation is swept. More specifically with reference to Fig. 1, an optically prepared beam of sodium atoms intersects at 90° the axis of a spherical mirror cavity formed by mirrors (m_a, m_b) each of radius 1 m. Two cavity configurations are employed; cavity *A* has a length of 1.7 mm and a finesse 18000, while cavity *B* has a length of 3.2 mm and a finesse which varied between 20000 and 26000 over a series of experiments. The particular transition investigated is the $(3S_{1/2}, F=2, m_F=2) \rightarrow (3P_{3/2}, F=3, m_F=3)$ transition at 589 nm. The cavity-plus-atoms system is excited by a signal field of carrier frequency ω_s which is matched to the TEM₀₀ cavity mode and onto which weak AM sidebands at frequency $\omega_s \pm \Omega_s$ have been generated by an electro-optic modulator. For fixed cavity detuning $\theta = (\omega_C - \omega_s)/\kappa$ and atomic detuning $\Delta \equiv (\omega_A - \omega_s)/\gamma_{\perp}$, the frequency Ω_s is swept and the Fourier components $x(\pm\Omega_s)$ of the field transmitted by the atom-cavity system are detected by optical heterodyning with an intense local oscillator of frequency $\omega_{LO} = \omega_s - \delta$ (with $\delta = 59.6$ MHz) in a balanced detector [photodiodes (D, D')]. More explicitly, for $\Omega_s < \delta$ the difference photocurrent, i in Fig. 1, contains coherent components at frequencies Ω_a

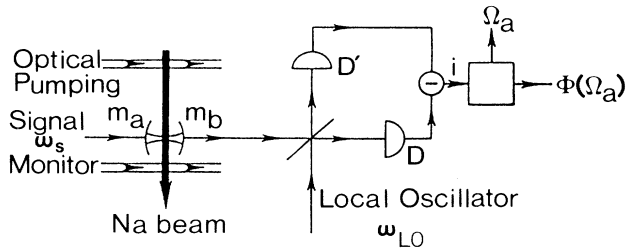


FIG. 1. Diagram of the apparatus as discussed in the text.

$= (\omega_s \pm \Omega_s) - \omega_{LO}$ corresponding to the coherent heterodyne beat between the local oscillator at ω_{LO} and the transmitted AM sidebands at $\omega_s \pm \Omega_s$. Hence from the spectral density of photocurrent fluctuations $\Phi(\Omega_a)$ obtained with an electronic spectrum analyzer, we are able to extract the quantity $|x(\pm\Omega_s)|^2$ after suitably accounting for the background (shot-noise) level and overall frequency dependence of the generation and detection system.

Transmission spectra acquired by this swept-sideband technique are presented in Fig. 2. Figure 2(a) is taken

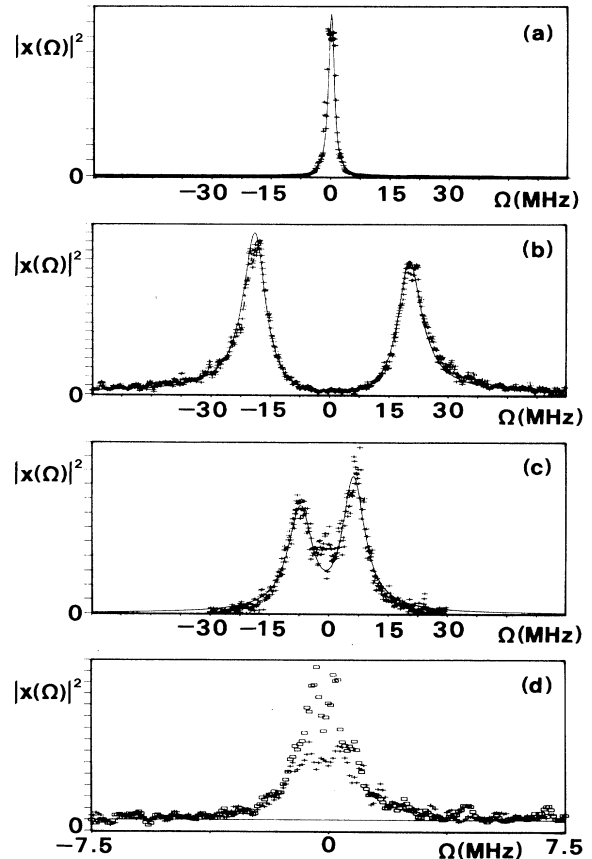


FIG. 2. Transmission spectra $|x(\Omega)|^2$ (arbitrary units) vs sideband frequency Ω , with $\Omega=0$ corresponding to the position of the carrier frequency at ω_s . Note that apart from an overall vertical scaling, all spectra are independent of the magnitude of x for $x \ll 1$. (a) Empty cavity ($C=0$) response with Lorentzian fit of 1.75 MHz FWHM. Cavity plus atoms for (b) $C=36$, $\Delta=-0.2$, $\theta \approx 0$, $\kappa/\gamma=0.09$; (c) $C=4.7$, $\Delta=0.1$, $\theta \approx 0$, $\kappa/\gamma=0.085$; (d) $\theta \approx 0$, $|\Delta| < 0.2$, displaying no splitting (overdamped regime) but with an increased linewidth and decreased peak transmission for the case of approximately 1 atom (+) compared to no atoms (\square) in the cavity. The full curves in (a)–(c) are obtained from the Maxwell-Bloch equations as discussed in the text, with + as our experimental points. The times to acquire the traces are (a)–(c) 0.7 s; (d) 20-trace average, 0.4 s per trace.

for an empty cavity ($C=0$) with $\theta=0$ and shows the measured response to the swept AM sidebands, together with a Lorentzian profile with $\kappa/2\pi=0.88$ MHz. Note that the origin for the abscissa has been placed at the frequency $\Omega_a=\delta$; therefore the rf spectra in Fig. 2 correspond to optical spectra displayed on an axis centered on the carrier frequency ω_s . Figures 2(b)–2(d) are transmission spectra for the composite atom-cavity system for weak-field excitation with the cavity servo-locked to the empty-cavity resonance ($\omega_C=\omega_s$) and the atomic detuning held close to zero ($\omega_A\cong\omega_s$). Clearly evident in Fig. 2(b) are spectral features offset from the empty-cavity response of Fig. 2(a); these peaks arise from the normal-mode splitting $\text{Im}(\lambda_{\pm})$ described by Eq. (1). The asymmetry between the peaks is accounted for by introducing a small atomic detuning ($|\Delta|<0.2$) corresponding to experimental uncertainties in the crossing angle between the cavity axis and the atomic beam direction and in laser frequency jitter. The spectra shown in Figs. 2(c) and 2(d) are taken for successively lower intracavity atomic numbers and illustrate the dependence of the normal-mode structure on the effective coupling rate $g\sqrt{N}$. In Fig. 2(c) the splitting is resolved for an effective intracavity number $N\sim 40$. Figure 2(d) is taken in the overdamped regime with $g\sqrt{N} < \frac{1}{4} |2\kappa - \gamma/\Gamma|$; for this trace, $N\sim 1$.

The solid lines in Figs. 2(b) and 2(c) are theoretical fits to the data obtained from the Maxwell-Bloch equations assuming $\theta=0$ and using the measured values of κ/γ and C (within their uncertainties), but allowing for

slight nonzero atomic detuning Δ as well as an overall scale factor. The atomic cooperativity parameter C and the required weak-field input are inferred from measurements on the hysteresis cycle of output versus input in absorptive bistability.¹⁶ We set $\Gamma=0.8$ to account phenomenologically for the combined effects of atomic transit and residual Doppler broadening. We stress that spectra such as those displayed in Fig. 2 are independent of the field amplitude x in the weak-field limit, as expected theoretically and confirmed experimentally.

From traces such as those in Fig. 2, we obtain a frequency splitting as well as a linewidth for each member of the doublet. In Fig. 3 we display an absolute comparison of the predicted splitting $\Omega_0\equiv\text{Im}(\lambda_{\pm})$ versus the measured splitting Ω_{exp} . There is reasonable agreement between theory and experiment over the range $20 < N < 600$ and for the two cavity configurations A and B . From linewidth measurements with cavity B in a regime in which the members of the split doublet are clearly resolved, we find widths for each of the components of the doublet of 7.5 ± 0.9 MHz, which is below both the free-space natural linewidth of 10 MHz for the Na transition and the ~ 13 -MHz absorption linewidth of the atomic beam due to transit and Doppler broadening. The theoretical full width for this comparison is given from Eq. (1) to be $(2\kappa + \gamma/\Gamma)/2$, which for $\kappa/\gamma=0.09\pm 0.01$, $\gamma/2\pi=10$ MHz, and $\Gamma=0.8$ yields a full width of 7.2 MHz.

Our discussion thus far has been restricted to the case of near resonance between atoms and cavity. We have inquired as well into the detuning dependence of the coupling-induced structure of the atom-field system, again in the weak-field limit. Clearly for $f\sim 10^{-5}$ as in our experiments, the eigenvalue structure should revert to that of independent atoms and cavity in the limit of large detuning. In Fig. 4 we present a comparison of experiment and theory (from the Maxwell-Bloch equations) for the dependence of the line position and linewidths on the cavity detuning θ for fixed atomic detuning $\Delta\cong 0$. For large θ and $\Delta=0$ the atoms and cavity are effectively decoupled, with corresponding eigenvalues $\lambda_1 = -(\kappa + i\theta)$ (empty cavity detuned by θ and damped at κ) and $\lambda_2 = -\gamma/2\Gamma$ (atoms driven on resonance with damping $\gamma/2\Gamma$), as indicated by the dashed lines in Fig. 4. However, as θ is decreased to zero, the eigenvalues are no longer those of the independent subsystems. In Fig. 4(a) the strong atom-field coupling results in a θ -dependent splitting Ω_{θ} (or avoided crossing) for the line positions. Likewise in Fig. 4(b) as $\theta\rightarrow 0$ the normal modes of the composite system are damped at a θ -dependent rate $\frac{1}{2}\beta_{\theta}$ rather than at the independent rates $(\kappa, \gamma/2\Gamma)$. In the terminology of cavity QED, Fig. 4 gives the detuning dependence of the vacuum radiative level shifts and linewidths of the composite atom-cavity system.

In summary, we have presented results from a spectroscopic study of a system of two-state atoms strongly cou-

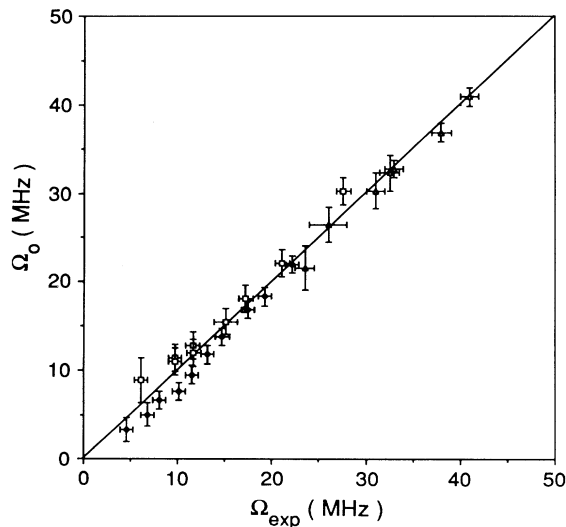


FIG. 3. Comparison of calculated normal-mode frequency $\Omega_0\equiv\text{Im}(\lambda_{\pm})$ vs measured splitting Ω_{exp} . All parameters that enter Ω_0 through Eq. (1) are known in absolute terms with the exception of Γ , which is chosen to be 0.8 to model phenomenologically the transit and Doppler broadening ($\Gamma=1$ radiative limit). Cavity A , $\kappa/\gamma=0.25$ (Δ); cavity B , $\kappa/\gamma=0.12$ (\square) and $\kappa/\gamma=0.09$ (\bullet).

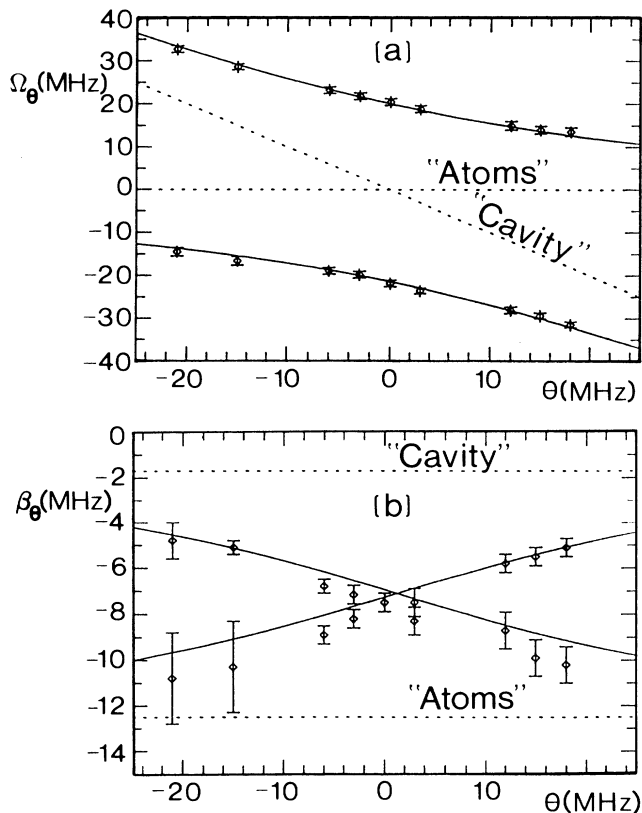


FIG. 4. Dependence of (a) normal-mode frequencies Ω_θ and (b) linewidths (FWHM) β_θ on cavity detuning θ for fixed atomic detuning $\Delta \cong 0$ in the weak-field limit. The data are obtained from traces similar to those in Fig. 2(b) with $C=41$, $\kappa/\gamma=0.085$. The full curves are the theoretical predictions for Ω_θ and β_θ obtained from the Maxwell-Bloch equations with these parameters and $\Gamma=0.8$; the dashed curves are for $g=0$ (uncoupled atoms and cavity).

pled to a single mode of an optical cavity. We have directly observed normal-mode splitting and subnatural linewidth averaging arising from the dynamical nature of the interaction of atoms and field. We infer from these measurements [Fig. 2(d)] that our method has the potential sensitivity to observe the splitting for a single atom in a cavity if the single-atom coupling coefficient g

can be made somewhat larger. We would then be in a position to address a number of questions relating to the nature of manifestly quantum or nonclassical dynamics in a dissipative setting.

This work was supported by the National Science Foundation (Grant No. PHY 8351074), by the Venture Research Unit of British Petroleum, and by the Office of Naval Research (Contract No. N00014-87-K-0156). M.G.R. gratefully acknowledges work support from IBM.

(a) On leave from Physics Department, University of Arkansas, Fayetteville, AK 72701.

¹S. Haroche and D. Kleppner, Phys. Today **42**, No. 1, 24 (1989), and references therein.

²E. M. Purcell, Phys. Rev. **69**, 681 (1946).

³D. Kleppner, Phys. Rev. Lett. **47**, 232 (1981).

⁴E. T. Jaynes and F. W. Cummings, Proc. IEEE **51**, 89 (1963).

⁵S. Haroche and J. M. Raimond, in *Advances in Atomic and Molecular Physics*, edited by D. Bates and B. Bederson (Academic, New York, 1985), Vol. 20, p. 347.

⁶G. Rempe, H. Walther, and N. Klein, Phys. Rev. Lett. **58**, 353 (1987); D. Meschede, H. Walther, and G. Muller, Phys. Rev. Lett. **54**, 551 (1985).

⁷M. Brune, J. M. Raimond, P. Goy, L. Davidovich, and S. Haroche, Phys. Rev. Lett. **59**, 1899 (1988).

⁸M. G. Raizen, R. J. Thompson, R. J. Brecha, H. J. Kimble, and H. J. Carmichael, in *Quantum Optics V*, edited by J. Harvey and D. F. Walls (Springer-Verlag, Berlin, 1989).

⁹R. J. Brecha, L. A. Orozco, M. G. Raizen, Min Xiao, and H. J. Kimble, J. Opt. Soc. Am. B **3**, 238 (1986).

¹⁰H. J. Carmichael, Phys. Rev. A **33**, 3262 (1986).

¹¹G. S. Agarwal, J. Opt. Soc. Am. B **2**, 480 (1985).

¹²J. J. Sanchez-Mondragon, N. B. Narozhny, and J. H. Eberly, Phys. Rev. Lett. **51**, 550 (1983).

¹³Y. Kaluzny, P. Goy, M. Gross, J. N. Raimond, and S. Haroche, Phys. Rev. Lett. **51**, 1175 (1983).

¹⁴H. J. Carmichael, R. J. Brecha, M. G. Raizen, H. J. Kimble, and P. R. Rice (to be published).

¹⁵G. S. Agarwal, Phys. Rev. Lett. **53**, 1732 (1984).

¹⁶L. A. Orozco, A. T. Rosenberger, and H. J. Kimble, Opt. Commun. **62**, 54 (1987).